Influence of Surface-Modifying Surfactants on the Pharmacokinetic Behavior of ^{14}C-Poly (Methylmethacrylate) Nanoparticles in Experimental Tumor Models

Jörg Lode,[1] Iduna Fichtner,[1] Jörg Kreuter,[2] Antje Berndt,[1] Julia Eva Diederichs,[1] and Regina Reszka[1,3]

Received June 27, 2001; accepted August 3, 2001

Purpose. The aim of this study was to investigate the different pharmacokinetic behavior of surface-modified poly(methylmethacrylate) (PMMA) nanoparticles.

Methods. The particles were ^{14}C-labeled and coated with polysorbate 80, poloxamer 407, and poloxamine 908. Plain particles served as control particles. *In vivo* studies were performed in three tumor models differing in growth, localization, and origin. Particle suspensions were administered via the tail vein, and at given time animals were killed and organs were dissected for determination of PMMA concentration.

Results. For the PMMA nanoparticles coated with poloxamer 407 or poloxamine 908, high and long-lasting concentrations were observed in the melanoma and at a lower level in the breast cancer model. In an intracerebrally growing glioma xenograft, the lowest concentrations that did not differ between the tumor-loaded and tumor-free hemispheres were measured. Organ distribution of the four investigated batches differed significantly. For instance, poloxamer 407- and poloxamine 908-coated particles circulated over a longer period of time in the blood, leading additionally to a higher tumor accumulation. In contrast, plain and polysorbate 80-coated particles accumulated mainly in the liver. The strong expression of vascular endothelial growth factor and Flk-1 in the melanoma correlated with high concentrations of PMMA in this tumor.

Conclusion. The degree of accumulation of PMMA nanoparticles in tumors depended on the particle surface properties and the specific growth differences of tumors.

KEY WORDS: poly(methylmethacrylate) (PMMA) nanoparticles; surface modification surfactant; *in vivo*; pharmacokinetics; angiogenesis; enhanced permeability and retention effect (EPR); tumor model.

INTRODUCTION

Macromolecular or colloidal drug carriers, such as polymer drug conjugates, liposomes, and nanoparticles, are gaining in importance for the therapy of solid tumors due to the enhanced permeability and retention (EPR) effect first described by Maeda and Matsumura (1,2). This effect, i.e., the observation that natural macromolecules, polymer-protein conjugates, and small particles accumulate passively in solid tumor tissue, has been attributed to two main factors (3,4). First, tumor vascularization often has a discontinuous endothelium, which allows macromolecular extravasion to a greater extent than via most other endothelial barriers, and second, these tumors also frequently display a lack of effective lymphatic drainage leading to macromolecular accumulation.

Moreover, angiogenesis has a profound influence on the amount of particles reaching the tumor and on the EPR effect. Jain (5) pointed out that angiogenesis (i) affects vascular permeability as well as the metabolic microenvironment, (ii) is different in tumors of various genesis, and (iii) greatly influences tumoral blood flow heterogeneity.

An additional factor seems to play an important role in the tumor accumulation of particulate drug carriers, namely, their surface properties. Beck *et al.* (6) and Reszka *et al.* (7) observed that the body distribution and the antitumoral effect of mitoxantrone differed in two different types of experimental tumors, leukemia P388 and B16-melanoma, depending on whether a drug carrier was used, as well as which type of carrier. The liposomes showed the highest antitumoral effects in leukemia P388, followed by the simple drug solution and, finally, the nanoparticles. In the solid B16-melanoma reversed results were observed: nanoparticles were most potent, a minor efficacy of the drug solution was revealed, whereas the liposomes were least effective. The two carriers differed in their surface properties. A number of authors, most extensively Tröster *et al.* (8), demonstrated previously in healthy animals that the body distribution of the nanoparticles after intravenous injection depended on their surface properties. These properties were monitored by the surfactants adsorbed onto the particles.

The objective of the present study was to investigate the influence of the surface properties on the transport of particles into different tumours. ^{14}C-poly(methylmethacrylate) (PMMA) nanoparticles were used in combination with three surfactants: polysorbate 80, poloxamer 407, and poloxamine 908. PMMA was chosen as a model polymer carrier material, because it can be ^{14}C-labeled within the polymer chain and because of its very slow biodegradability. These properties enable an accurate determination of the body distribution of virtually nondegraded carriers for more than 1 week (9). Uncoated nanoparticles served as control particles. Three tumor models were chosen: the murine B16-melanoma as well as a human breast cancer (MaTu) and a human glioblastoma (U-373) transplanted into nude mice. The latter tumor was selected because we wanted to know whether the particles, or at least the particle-bound drugs, are able to cross one of the tightest barriers for drug delivery, the blood-brain barrier (10–13). This barrier also may become leaky in later stages of tumor development but represents a major obstacle at least in the initial phase. The expression of vascular endothelial growth factor (VEGF) and FLK-1 in the tumor models was investigated to characterize the different tumors according to vasculature parameters and to find an explanation for the nanoparticle accumulation in the tumor models.

[1] Max-Delbrück-Center for Molecular Medicine, Robert-Rössle-Str. 10, 13122 Berlin, Germany.

[2] Institute of Pharmaceutical Technology, J. W. Goethe-Universität, Biozentrum, Marie-Curie-Str. 9, Frankfurt/Main.

[3] To whom correspondence should be addressed. (e-mail: RESZKA@MDC-BERLIN.DE)

ABBREVIATIONS: PMMA, polymethylmethacrylate; AUC, area under the curve; Cl, clearance; V_d, volume of distribution; EPR, enhanced permeability and retention effect; VEGF, vascular endothelial growth factor; Flk-1, fetal liver kinase-1; RES, reticuloendothelial system.

0724-8741/01/1100-1613$19.50/0

MATERIALS AND METHODS

Preparation of ^{14}C-Labeled Nanoparticles

Radioactive monomer methyl(2-^{14}C)methacrylate customer-synthesized by Amersham Radiochemical Centre (Buckinghamshire, UK) was used for the preparation of the nanoparticles carried out by gamma irradiation-induced polymerization as described elsewhere (14). The particle suspension was freeze-dried as a suspension in 0.15 M phosphate-buffered saline. The lyophilized powder contained 37.2% polymethylmethacrylate and 62.8% buffer salt [dibasic sodium phosphate dihydrate-monobasic potassium phosphate-sodium chloride (7.6:1.45:4.8; w/w/w)]. The lyophylisate possessed an activity of 4.43 μCi/mg.

Particle size determination by laser light diffraction (LS230, Coulter Technices, Miami, FL) showed the same median value of 107 nm for the uncoated and coated particles after incubation in human plasma for 5 min. The size of the particle diameter measured by electron microscopy was on the same order of magnitude as detected with laser light diffraction. The particles used were stable over the entire time of experiments *in vivo* (14).

Surfactants

Three different surfactants were used to modify the surface of the nanoparticles: polysorbate 80 (Tween 80; Sigma, Göttingen, Germany), poloxamer 407 (Pluronic F127; Erbslöh, Krefeld, Germany), and poloxamine 908 (Tetronic 908; BASF, Mount Olive, New Jersey).

Preparation of the Suspension for Intravenous Administration

Uncoated batch (*A*): The lyophilized PMMA-buffer salt-mixture (30.34 mg) was resuspended in 10 mL distilled water and ultrasonicated at 35 kHz (Ultrasonicator T570, Roth, Karlsruhe, Germany) for 20 min.

Coated batches (*B, C, D*): The PMMA-containing lyophylisate (30.34 mg) was added to 5 mL distilled water and ultrasonicated; after 5 min, a 2% surfactant solution (5 mL) was added to receive a 1% mixture. Thereafter, the suspensions were processed like the uncoated batch for another 15 min.

The resulting suspensions of uncoated and coated PMMA nanoparticles for i.v. administration had a final concentration of 1.128 mg PMMA/mL medium and were termed as follows: *A*: PMMA uncoated; *B*: PMMA coated with polysorbate 80; *C*: PMMA coated with poloxamer 407; *D*: PMMA coated with poloxamine 908.

Activity of the Suspensions

The specific activities of the suspensions of the coated batches and the uncoated batch were evaluated. For that purpose, four samples of each batch in each trial were mixed with scintillation cocktail (Ready Organic Cocktail, Beckman Instruments GmbH, Munich, Germany) and counted in a liquid scintillation counter (TRI-CARB/1900TR, Packard, Groningen, Netherlands) as described below. The nanoparticle suspensions were prepared freshly for each experiment (Table I). The average activity of all suspensions was 5.08 ± 0.87 μCi/mL.

Animals and Tumor Models

For the melanoma model, female B6D2F1 mice (Charles River, Sulzfeld, Germany) were used, and for both other models (breast cancer, glioblastoma) female nude mice (Ncr, Taconic, Germantown, PA) were used. The B6D2F1 mice were kept at room temperature (20°C), nude mice at 25°C and a relative humidity of 50% The animals received sterilized water and diet (Ssniff, Soest, Germany) *ad libidum.* All investigations using experimental animals adhered to the "Principles of Laboratory Animal Care" (NIH publication #85-23, revised 1985).

Murine B16-melanoma was inoculated as a tumor homogenate (0.5×10^6 cells in 0.1 mL) intramuscularly (i.m.) into 160 B6D2F1 mice on day 0. On day 14 the tumors had an average weight of 1110 mg (SD ± 660 mg).

The cells (1×10^7) of the human breast cancer MaTu were administered subcutaneously (s.c.) into 160 nude mice, and the tumors reached a weight of 259 mg (SD ± 186 mg) by treatment day 21.

The human U-373 glioblastoma cells (2×10^5 cells) were administered intracerebrally (i.cer.) in 134 nude mice with a 10-μL Hamilton syringe (Hamilton, Sigma, Göttingen, Germany) in a volume of 3 μL with the help of a stereotactic device. Before injections, a hole was drilled into the scull 3 mm beside the median line on the bregma. The tumor cell administration was performed 3 mm deep in the putamen during a time period of 5 min. On the day of nanoparticle treatment (day 18) four randomized animals were killed; the brain was dissected, shock-frozen (–40°C), sliced (5 μm), and stained with Kresylviolett (Merck, Darmstadt, Germany) to detect the size of the glioblastoma. The average glioblastoma volume was 2.24 mm^3 (SD ± 0.08 mm^3) on the day of treatment.

Injection

For each nanoparticle group (*A, B, C, D*) four (glioblastoma model) or five animals (B16–melanoma- and MaTu-breast cancer model) at each time point (0.5, 1, 2, 4, 8, 24, 72, and 168 h) were used. All mice obtained an adequate volume (0.01 mL/g body weight) of suspension administered via the tail vein at a rate of 1 mL/min. Because of rapid aggregation

Table I. Specific Radioactivity ± SD of Each PMMA Suspension

Trial	*A* [μCi/mL]	*B* [μCi/mL]	*C* [μCi/mL]	*D* [μCi/mL]
1. Melanoma model	5.98 ± 0.01	5.14 ± 0.08	5.09 ± 0.07	4.30 ± 0.26
2. Breast cancer model	7.31 ± 0.12	4.05 ± 0.05	4.63 ± 0.06	5.11 ± 0.26
3. Glioblastoma model	4.62 ± 0.22	4.02 ± 0.04	5.56 ± 0.21	5.12 ± 0.17

A: PMMA uncoated; *B*: PMMA coated with polysorbate 80; *C*: PMMA coated with poloxamer 407; *D*: PMMA coated with poloxamin 908.

of the uncoated nanoparticles, it was necessary to ultrasonicate the particle suspension for 20 s immediately before use.

Preparation of Organs

At the indicated time points, blood (0.1 mL) was taken from the retro-orbital venous plexus, and the animals were killed by cervical dislocation and passively exsanguinated. After opening the abdomen and the chest, the liver, spleen, kidneys, lung, heart, and brain were dissected. The breast cancer and the melanoma nodules were removed completely from the healthy tissue. All organs were weighed immediately after removing and stored in glass vials at –20°C. The glioblastoma could not be dissected from the brain, because of its soft consistency. Therefore, the tumor-free and the tumor-bearing brain hemispheres were collected separately. The tail was also examined by using the same conditions as for the other tissue samples.

Determination of the ^{14}C-Radioactivity

After thawing of the organs, 1-mL tissue solubilizer (BTS-450; Beckman Instruments GmbH) was added, and the samples were stored at room temperature for 1–2 days. After a complete tissue solubilization 0.1–0.3 mL H_2O_2 (30%) was added for destaining. The glass vials were filled up with 10 mL scintillation cocktail (Ready Organic Cocktail, Beckman Instruments GmbH), stored 2 weeks in the dark, and thereafter counted in a liquid scintillation counter (TRI-CARB/1900TR, Packard) for a decline of inherent chemoluminescence.

Calculation of the PMMA Concentration in the Organs

The evaluation of the activity in the blood, in the organs, and tumors was performed after subtraction of the radioactivity in the tail from the total administered dose. The concentrations (ng PMMA) of the nanoparticle preparations were evaluated per mg tissue weight for a better interexperimental comparability of the PMMA concentrations. An average value of 6.6% of total body weight was used for the calculation of blood volume.

Data Analysis

All data were expressed as median and quartiles (25th and 75th percentiles), because of the nonparametric distribution of the data. For statistical calculations, the software program STATISTICA 5.0, including the nonparametric *U*-test of Mann and Whitney with a significance level of $P \leqslant 0.05$, was used.

The blood values were analyzed on the basis of a three-compartment system with a pharmacokinetic software (TOPFIT 2.1). With that model, the best adaptation of the software calculated curve to the measured values was obtained. The area under the curve (AUC), the clearance (Cl), and the volume of distribution (V_d) were calculated.

Immunohistologic Staining

The three tumors used were investigated with regard to their ability to induce angiogenesis. The immunohistologic investigation was performed on separate tumor samples excised at the same time when the mice were treated with the nanoparticles. After the samples were sliced (5 μm) and air-dried, an antibody against the VEGF (Cl) (Santa Cruz Biotechnology, Heidelberg, Germany) and an antibody detecting the VEGF receptor FLK-1 (A-3) (Santa Cruz Biotechnology) were used. The immunohistologic staining was performed with the LSAB-2Kit (K677; Dako, Hamburg, Germany) according to a routine protocol (Dako); hämalaun was chosen as the counterstaining agent. The slices were evaluated by counting 400 cells with light microscopy (Axioskop, Zeiss, Jena, Germany).

RESULTS

The body distribution of uncoated and coated PMMA nanoparticles was investigated after i.v. administration in tumor-bearing mice during a period of 168 h. Three different *in vivo* models were chosen to ensure relatively broad information on the ability of plain and surface-modified nanoparticles to achieve high concentrations in a variety of tumorous tissue. Tumors different in growth, localization, and origin were used. The average weight of the murine melanoma on the day of particle injection was 4 times higher than the weight of the human breast cancer nodules. As a third model, an intracerebrally growing glioblastoma was selected.

For the PMMA nanoparticles coated with the surfactants poloxamer 407 or poloxamine 908, high and long-lasting concentrations were observed in two tumor models (Table II). The other preparations (uncoated and coated with polysorbate 80 PMMA) were not able to induce remarkable concentrations in tumor tissue.

In the melanoma (first trial) 2 h after i.v. injection, a maximum of 23.4 ng nanoparticles per mg was found for batch *C* and of 21.4 ng per mg tumor tissue for batch *D* (Table II), corresponding to 14.5% and 15.6% of the total nanoparticle dose (data not shown). We observed a fast and continued increase of radioactivity after injection of batches *C* and *D* during the first 2 h. That was followed by a slow decrease with a second peak measured 24 h after administration (20.38 and 18.85 ng/mg tumor tissue for batches *C* and *D*). Hence, sufficiently high concentrations in the tumor during more than 24 h were maintained, although the particle concentrations in the blood decreased exponentially (Fig. 1a). In comparison, within the other investigated organs, relatively high concentrations of particles were found only in the liver and the spleen during the total investigation time.

In the second trial (breast cancer), the maximum concentrations (Table II) were clearly lower compared to the melanoma, but the proportional accumulation of the different nanoparticle batches was the same as in the first trial. Again, batches *C* and *D* achieved the highest radioactivity in the human breast cancer xenografts. The PMMA concentrations of these batches were relatively stable during the time of investigation. At the last time point (168 h) the concentrations of batches *C* and *D* were at least 10-fold higher than in the melanoma trial.

In the third trial, the enrichment of plain and coated PMMA nanoparticles was measured in a glioma model. None of the formulations could produce a higher concentration in the tumor-bearing than in the tumor-free brain hemisphere (Fig. 2). Only among the particle formulations were differences observed. The highest concentrations were achieved after administering batches *C* and *D* (in all three trials) between 0.5 and 1 h, but the values were always below 0.5% of the total administered dose.

Table II. Concentration of PMMA in Tumor Tissue (ng/mg) (Trial 1 and 2) as Median Values with Q25 (25th Percentiles) and Q75 (75th Percentiles)

		B16-melanoma			MaTu breast cancer		
Time (h)	Group	Median value	Q25	Q75	Median value	Q25	Q75
0.5	*A*	**3.43**	1.97	6.33	**0.92**	0.47	1.65
	B	**0.95**	0.88	4.22	**1.27**	0.81	1.47
	C	**11.89**	10.17	12.70	**2.13**	1.86	3.06
	D	**6.94**	5.12	18.25	**2.78**	2.65	2.96
1	*A*	**0.61**	0.58	0.73	**0.62**	0.50	0.65
	B	**1.58**	1.27	3.22	**0.68**	0.49	0.93
	C	**11.20**	10.20	13.38	**1.82**	1.61	2.37
	D	**9.81**	8.88	12.25	**2.37**	2.31	2.56
2	*A*	**1.41**	0.99	7.48	**0.95**	0.93	1.30
	B	**2.16**	1.77	3.95	**0.67**	0.57	0.75
	C	**23.42**	11.69	34.14	**2.34**	2.16	2.50
	D	**21.36**	5.30	21.46	**3.15**	2.88	3.46
4	*A*	**1.54**	1.25	1.78	**0.61**	0.54	1.24
	B	**1.76**	0.64	2.27	**0.50**	0.19	0.51
	C	**13.77**	13.77	28.33	**3.13**	2.58	3.95
	D	**15.87**	12.08	19.80	**4.29**	3.08	6.82
8	*A*	**0.80**	0.73	1.15	**1.12**	0.72	1.49
	B	**3.14**	1.27	3.52	**0.56**	0.51	1.62
	C	**15.23**	10.98	15.46	**3.41**	3.10	3.74
	D	**14.56**	9.06	15.81	**3.11**	2.97	4.39
24	*A*	**0.76**	0.48	0.95	**0.49**	0.40	0.81
	B	**2.80**	1.43	3.77	**0.76**	0.35	0.95
	C	**20.38**	8.12	26.44	**4.24**	3.96	4.30
	D	**18.85**	13.56	21.85	**3.36**	2.54	4.64
72	*A*	**0.49**	0.47	1.26	**0.54**	0.47	0.74
	B	**0.88**	0.57	1.11	**0.20**	0.16	0.25
	C	**7.84**	4.64	10.37	**2.34**	1.83	2.48
	D	**5.71**	5.69	5.97	**5.24**	4.48	5.60
168	*A*	**0.61**	0.35	0.92	**0.25**	0.20	0.30
	B	**0.13**	0.06	0.15	**0.25**	0.20	0.82
	C	**0.27**	0.19	0.44	**2.63**	1.82	3.73
	D	**0.21**	0.00	0.60	**4.12**	3.46	4.89

A: PMMA uncoated; *B*: PMMA coated with polysorbate 80; *C*: PMMA coated with poloxamer 407; *D*: PMMA coated with poloxamin 908.

All three tumors were investigated with regard to their ability to express VEGF and FLK-1. In the fast-growing B16-melanoma a high and widespread expression of VEGF and of Flk-1 was found (Table III). In the breast cancer, a lower expression than in the melanoma was observed for both proteins. In the glioblastoma, no stained cells could be found.

For the nanoparticles coated with poloxamer 407 and poloxamine 908, a high and long-lasting concentration in the blood (Fig. 1a) was observed. At 0.5 h after i.v. administration, concentrations of 103,531 ng PMMA per mL blood for batch *C* and of 89,301 ng PMMA per mL blood for batch *D,* corresponding to 60 and 61% of the total dose of the poloxamer 407 and poloxamine 908-coated PMMA nanoparticles, respectively, were found. The blood concentrations of batches *C* and *D* were significantly higher, up to 8 h, than the concentrations of *A* and *B*. Also after 8 h of circulation, 11,326 (batch *C*) and 18,590 (batch *D*) ng per mL blood, corresponding to 6–12% of the total dose were registered. In the second trial, we also investigated the concentration of the particles 5 min after i.v. administration; only 3.5% for batch *A* and 9.6% for batch *B* of the total dose could be found in the blood at that time point. The clear differences beween the particle formulations were underlined by the pharmacokinetic calculations (Table IV). The AUC of batches *C* and *D* was more than 100 times higher than the AUC of the batches *A* and *B*.

In the liver, we observed a high and relatively constant concentration of 150–200 ng PMMA per mg tissue (Fig. 1b) over the total time period corresponding to 57–71% of the total administered dose for the plain and the polysorbate 80-coated PMMA nanoparticles. In contrast, the concentrations of batches *C* and *D* were much lower, but increased continuously.

In the spleen, an opposite group ranking compared to the liver was found (Fig. 1c). The particles, which led to high radioactivity in the liver, were found in low levels in the spleen. Especially remarkable is the increase of spleen concentrations during prolonged times for preparations *C* and *D,* whereas the levels for preparations *A* and *B* remained relatively constant. The highest concentration was detected in the spleen with 1,539 ng per mg tissue for batch *C* 168 h after injection. This is the highest concentration ever detected in any of the investigated organs.

The courses of the PMMA radioactivity and the group ranking in the brain (Fig. 1d), lung, and kidney (data not shown) resembled each other. In the kidney, we measured a maximum at the first time point (0.5 h) after the i.v. administration of the particle formulations and afterward an exponential decline. In the brain and in the lung, the maximum was detected at 1 or 2 h after treatment with a similar elimination behavior. In most organs, only a low level of polysorbate 80-coated PMMA nanoparticles was found.

DISCUSSION

The objective of our study was the evaluation of the influence of surface-modifying surfactants on the body distribution of PMMA nanoparticles in tumor-bearing mice. These preparations were previously tested for their pharmacokinetic behavior and tissue distribution in rats by Tröster *et al.* (8). Poloxamer 407 and poloxamine 908 are especially well investigated surface-modifying surfactants for nanoparticles. Poloxamine 908 is known to increase the blood circulation time and to reduce the uptake of nanoparticles in the liver (6,8). Some authors (10–13) reported that polysorbate 80-coated nanoparticles were able to overcome the blood-brain barrier. Consequently, this surfactant was also chosen to coat the PMMA nanoparticles and to examine its ability to achieve an enrichment in different tumor types.

The maximum concentrations of 23.4 ng per mg tumor tissue for batch *C* and of 21.4 ng for batch *D* determined in the present study are difficult to compare with most data from the literature, because these authors investigated the effect of cytostatics loaded to nanoparticles on tumor size, survival rate, and toxic side effects (15–17). In the few studies reporting drug concentrations in tumors their maxima varied from 1.4% (18) on day 14 in a human osteosarcoma up to 12% (7) of the total dose at 1 h in a B16-melanoma. In our trials, we

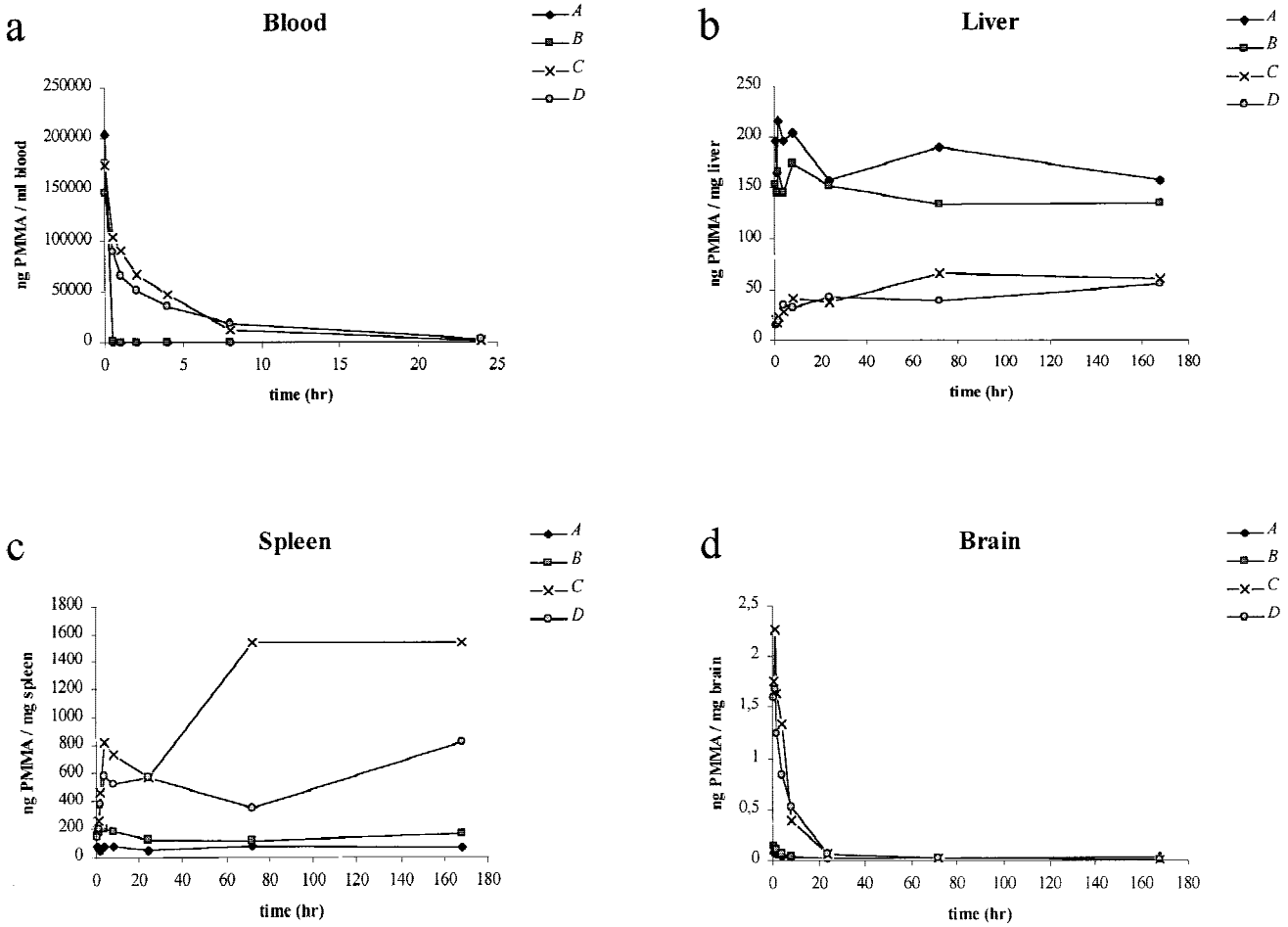

Fig. 1. Concentration of PMMA nanoparticle preparations in blood (a), liver (b), spleen (c), and brain (d) (trial 1) over time after i.v. administration. The particle concentrations in groups *C* and *D* were significantly different from the concentrations of groups *A* and *B* (for details see text). Median values of four to five mice were determined per time point. *A*: PMMA uncoated; *B*: PMMA coated with polysorbate 80; *C*: PMMA coated with poloxamer 407; *D*: PMMA coated with poloxamin 908.

found 14.5% for batch *C* and 15.5% of the total dose for batch *D* in the B16 melanoma 2 h after i.v. application. In the MaTu breast cancer the maximum concentration was clearly lower than in the melanoma. A possible reason for the lower accumulation of batches *A* and *B* may be the very low blood circulation time for those preparations in all trials. After 5 min (trial 2) 91–96% of the dose was apparently removed from the blood, probably by the cells of the RES and mainly accumulated in the liver. The difference between both tumors could be related to individual tumor tissue properties, e.g., to tumor-associated angiogenesis. The strong expression of VEGF and Flk-1 in the melanoma correlated with high concentrations of PMMA in this tumor. Interactions of the vascular growth factor and the receptor of endothelial cell membranes led to induction of angiogenesis in this tumor. The tumor-associated vasculature has typical peculiarities such as strong fenestration in the vessels, incomplete basal membranes (19), and a higher endocytotic activity of endothelial cells (20). Maeda *et al.* (1,2) described and summarized this phenomenon as the EPR effect and as a reason for the accumulation of colloidal carriers such as liposomes and nanoparticles in solid tumors.

The results in the glioblastoma model revealed no differences between tumor-free and tumor-bearing brain hemispheres. A remaining intact blood-tumor barrier could be discussed as the reason for that observation. Such a barrier is developed in intracerebrally growing tumors, not in s.c. inoculated malignancies (5). Polysorbate 80 was described as a very efficient surfactant to overcome the barrier (10–13). However, in our experiments with PMMA this was not confirmed. A reason could be that the cited authors used another nanoparticle formulation [poly-(butylcyanoacrylate)]. A lack of VEGF and Flk-1 expression in the glioma could also be responsible for the failed accumulation of PMMA particles in the malignant tissue. It is well known from clinical data that human glioblastomas grow in patients over a long period of time and induce a profound angiogenesis. Because of ethical reasons and experimental limitations, we used a xenograft growing only for 18 days before treatment. Therefore, this model probably does not exactly reflect the human conditions concerning mainly more advanced tumor stages.

The blood circulation time was similar in all three trials for the PMMA formulations. Batches *C* and *D* circulated consistently in high and long-lasting concentrations. Tröster *et al.* (8), who worked with the same nanoparticles and the same surfactants, but with a slightly modified preparation protocol, reported somewhat different circulation times. Dunn *et al.* (21) pointed out that with the same surfactants onto polysty-

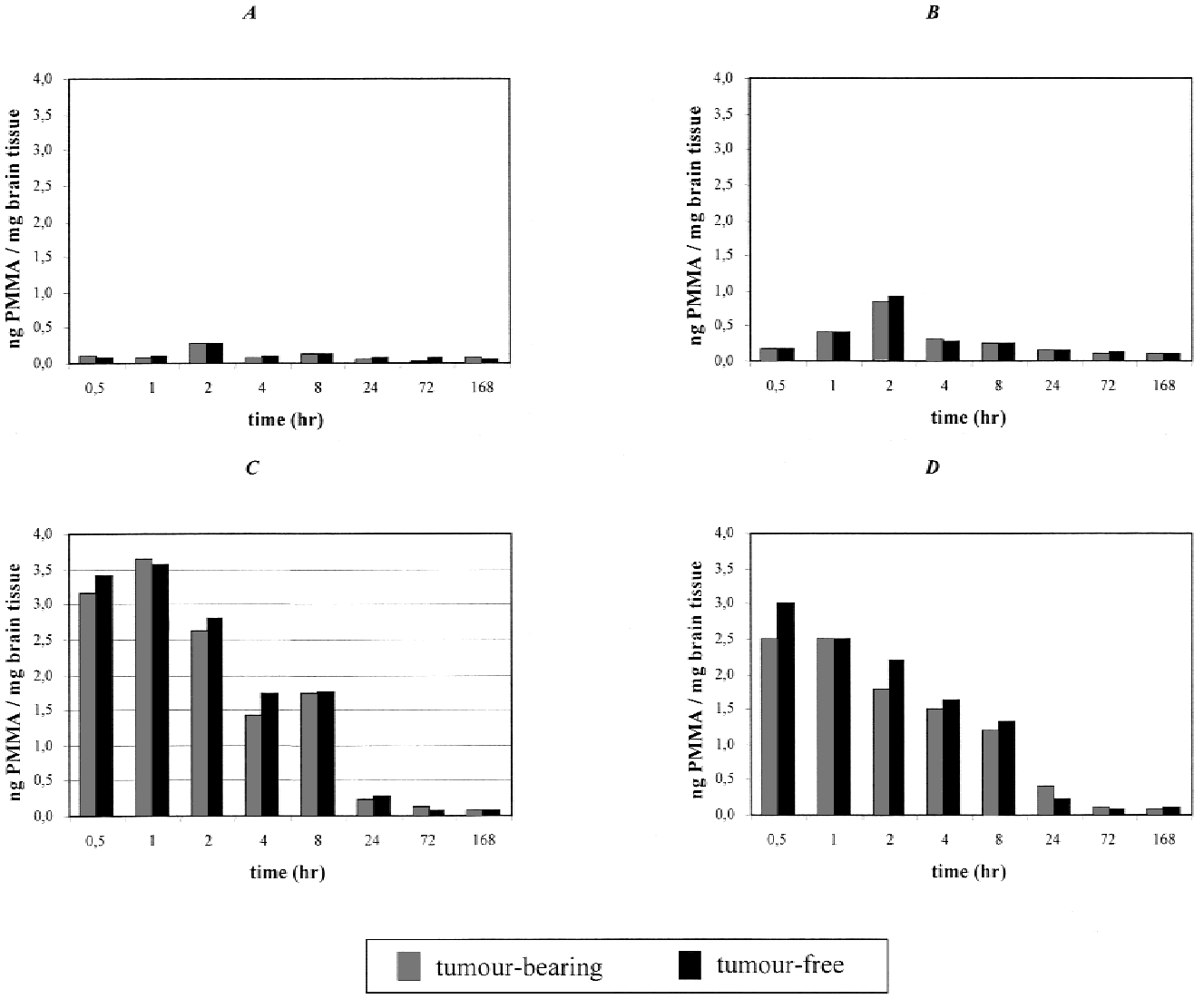

Fig. 2. PMMA concentrations in ng/mg in tumor-free and tumor-bearing brain-hemisphere (trial 3) after i.v. administration. *A*: PMMA uncoated; *B*: PMMA coated with polysorbate 80; *C*: PMMA coated with poloxamer 407; *D*: PMMA coated with poloxamin 908.

rol and poly-lactide-co-glycolide nanoparticles, maximum blood concentrations of 39 and 28%, respectively, of the total dose after 3 h were achieved in rats, whereas in rabbits only poloxamer 407-coated poly-lactide-co-glycolide nanoparticles circulated for a prolonged time but not those coated with other surfactants.

In our experiments, the PMMA concentration in the lung never exceeded 2.6% of the total dose (data not shown). In contrast, Tröster *et al.* (8) found maximum concentrations of 42% of the total dose for poloxamer 407-coated PMMA nanoparticles in the lung. These differences in the lung concentrations probably result from different preparation protocols and suggest that our particles probably lack the potential of lung embolism.

The particle formulations with the lowest values in the blood showed the highest level in the liver (Fig. 1a and b). The liver is the main collecting organ for plain and polysor-

Table III. Immunohistologic Examination of VEGF and Flk-1

Tumor	VEGF	VEGF-receptor (Flk-1)
B16-melanoma	++	++
MaTu-breast cancer	+	+
U373-glioblastoma	—	—

—, no stained cells per 4 × 100 counted cells per slide.
+, 2–5 stained cells per 4 × 100 counted cells per slide.
++, 5–10 stained cells per 4 × 100 counted cells per slide.

Table IV. Pharmacokinetic Parameters according to a Three-Compartment Model from Blood Values (Trial 1)

Nanoparticle preparation	AUC [ng/mL * h]	Cl [mL/min]	V_d [mL]
A	3,790	0.0594	0.332
B	4,470	0.0433	0.299
C	725,000	0.000264	0.0000539
D	446,000	0.000363	0.0832

A: PMMA uncoated; *B*: PMMA coated with polysorbate 80; *C*: PMMA coated with poloxamer 407; *D*: PMMA coated with poloxamin 908.

bate-80-coated PMMA particles. The liver is well prepared to take up vesicular material such as nanoparticles, liposomes, and microcapsules because of the function of the liver: (i) massive blood flow, (ii) strongly fenestrated capillaries, and (iii) a high number of Kupffer cells (22). Surfactants are able to change the surface properties in such a way that the phagocytosis by cells of the RES is reduced as the particles are apparently "masked." In our experiments, only poloxamer 407 and poloxamine 908 were able to decrease the uptake in the liver.

In contrast to liver, spleen, and tumor, in the other organs such as brain (Fig. 1d), kidney, and heart (data not shown), a high concentration of particles was found immediately after administration with a rapid decrease at later time points. This could be due to a reversible adhesion of the particles to the vessel walls and not a real uptake into the tissues.

In conclusion, our study showed that poloxamer 407- and poloxamine 908-coated PMMA nanoparticles are able to accumulate in tumor tissue. For these formulations, we also observed a long-lasting blood circulation and a reduction of the liver uptake compared with the uncoated and the polysorbate-80 PMMA particles. PMMA concentrations in the melanoma and the breast cancer models were significantly higher for groups *C* and *D* compared with groups *A* and *B*. There was a clear difference between the tumor models, the tumor (melanoma) with the highest expression of VEGF and FLK-1, and the highest growth rate showed a 4- to 5-times higher accumulation of PMMA nanoparticles compared with the other malignancies. It is of interest that no distinction with regard to accumulation of nanoparticles was observed between normal brain tissue and glioblastoma growing intracerebrally. Our results demonstrate that the surface-modified nanoparticles are not able to overcome the blood-brain barrier. It is necessary to investigate in further studies whether drugs encapsulated or associated with surface-modified nanoparticles can cross the blood-brain barrier either after release from the particles or in particle-associated form. These results are in good correlation with the immunhistochemical experiments, because no angiogenesis-related markers could be found in the brain tumor xenografts.

ACKNOWLEDGMENTS

This study was supported by a grant from the German Research Foundation (Deutsche Forschungsgemeinschaft DFG) Kr-867/10-1. The authors thank Mrs. M. Becker and Mrs. M. Lemm, whose technical assistance was highly appreciated. We also thank Dr. J. E. Diederichs for critical reading of the manuscript.

REFERENCES

1. Y. Matsumura and H. Maeda. A new concept for macromolecular therapeutics in cancer chemotherapy: mechanism of tumoritropic accumulation of proteins and the antitumor agent SMANCS. *Cancer Res.* **6**:6387–6392 (1986).
2. H. Maeda and Y. Matsumura. Tumoritropic and lymphotropic principles of macromolecular drugs. *CRC Crit. Rev. Ther. Drug Carrier Syst.* **6**:193–210 (1989).
3. L. W. Seymour. Passive tumour targeting of soluble macromolecules and drug conjugates. *CRC Crit. Rev. Ther. Drug Carrier Syst.* **9**:135–187 (1992).
4. R. Duncan, S. Dimitijevic, and E. G. Evagorou. The role of polymer conjugates in the diagnosis and treatment of cancer. *S.T.P. Pharma Sci.* **6**:237–263 (1996).
5. R. K. Jain. Delivery of molecular and cellular medicine to solid tumors. *Microcirculation* **4**:1–23 (1997).
6. P. Beck, J. Kreuter, R. Reszka, and I. Fichtner. Influence of polybutylcyanoacrylate nanoparticles and liposomes on the efficacy and toxicity of the anticancer drug mitoxantrone in murine tumor models. *J. Microencapsul.* **10**:101–114 (1993).
7. R. Reszka, P. Beck, I. Fichtner, M. Hentschel, J. Richter, and J. Kreuter. Body distribution of free, liposomal and nanoparticle-associated mitoxantrone in B16-Melanoma-bearing mice. *J. Pharmacol. Exp. Ther.* **280**:232–237 (1997).
8. S. D. Tröster, K. H. Wallis, R. H. Müller, and J. Kreuter. Correlation of the surface hydrophobicity of ^{14}C-poly(methyl methacrylate) nanoparticles to their body distribution. *J. Control. Release* **20**:247–260 (1992).
9. S. D. Tröster and J. Kreuter. Influence of the surface properties of low contact angle surfactants on the body distribution of ^{14}C-poly(methyl methacrylate) nanoparticles. *J. Microencapsulation* **9**:19–28 (1992).
10. U. Schröder and B. A. Sabel. Nanoparticles, a drug carrier system to pass the blood-brain barrier, permit central analgesic effects of i.v. dalargin injections. *Brain Res.* **710**:121–124 (1996).
11. J. Kreuter, R. N. Alyautdin, D. A. Kharkevich, and A. A. Ivanov. Passage of peptides through the blood-brain barrier with colloidal polymer particles (nanoparticles). *Brain Res.* **674**:171–174 (1995).
12. R. N. Alyautdin, D. Gothier, V. E. Petrov, D. A. Kharkevich, and J. Kreuter. Analgesic activity of the hexapeptide dalargin adsorbed on the surface of polysorbate 80-coated poly(butylcyanoacrylate) nanoparticles. *Eur. J. Pharm. Biopharm.* **41**:44–48 (1995).
13. R. N. Alyautdin, V. E. Petrov, K. Langer, A. Berthold, D. A. Kharkevich, and J. Kreuter. Delivery of loperamid across the blood-brain barrier with polysorbate 80-coated poly-butylcyanoacrylate nanoparticles. *J. Pharm. Res.* **14**:325–328 (1997).
14. J. Kreuter, U. Täuber, and V. Illi. Distribution and elimination of poly(methyl-2-^{14}C-methacrylate) nanoparticle radioactivity after injection in rats and mice. *J. Pharm. Sci.* **68**:1443–1447 (1979).
15. F. Brasseur, P. Couvreur, B. Kante, L. Deckers-Passau, M. Roland, C. Deckers, and P. Speiser. Actinomycin D adsorbed on polymethylmethacrylate nanoparticles: an increased efficiency against an experimental tumor. *Eur. J. Cancer* **16**:1441–1445 (1980).
16. P. Couvreur, L. Grislain, and V. Lenaerts. Biodegradable polymeric nanoparticles as a drug carrier for antitumor agents. In P. Guiot and P. Couvreur (eds.), *Polymeric Nanoparticles and Microspheres,* CRC Press, Boca Raton, 1986.
17. D. Sharma, T. Chelvi, J. Kaur, K. Chakravorty, T. De, A. Maitra, and R. Ralham. Novel Taxol® formulation: polyvinylpyrolidone nanoparticle-encapsulated Taxol® for drug delivery in cancer therapy. *Oncol. Res.* **8**:281–286 (1996).
18. E. M. Gipps, R. Arshady, J. Kreuter, P. Groscurth, and P. P. Speiser. Distribution of polyhexylcyanoacrylate nanoparticles in nude mice bearing human osteosarcoma. *J. Pharm. Sci.* **75**:256–258 (1986).
19. B. Endrich, H. S. Reinhold, J. F. Gross, and M. Intaglietta. Tissue perfusion inhomogeneity during early tumor growth in rats. *J. Natl. Cancer Inst.* **62**:387–395 (1979).
20. J. Kreuter. Drug targeting with nanoparticles. *Eur. J. Drug Metab. Pharmacokinet.* **3**:253–256 (1994).
21. S. E. Dunn, A. G. A. Coombes, M. C. Garnett, S. S. Davis, M. C. Davies, and L. Illum. In vitro cell interaction and in vivo biodistribution of poly (lactide-co-glycolide) nanospheres surface modified by poloxamer and poloxamine copolymers. *J. Control. Release* **44**:65–76 (1997).
22. J. E. O'Mullane, P. Artursson, and E. Tomlinson. Biopharmaceutics of microparticle drug carriers. *Ann. NY Acad. Sci.* **507**:100–140 (1987).